Dimeric Fcγ Receptor Enzyme-Linked Immunosorbent Assay To Study HIV-Specific Antibodies: A New Look into Breadth of Fcγ Receptor Antibodies Induced by the RV144 Vaccine Trial

Milla R. McLean,* Vijaya Madhavi,* Bruce D. Wines,[†,‡,§] P. Mark Hogarth,[†,‡,§] Amy W. Chung,*[,1] and Stephen J. Kent*[,¶,‖,1]

Ab-dependent cellular cytotoxicity (ADCC) responses are of growing interest in the HIV vaccine field but current cell-based assays are usually difficult to reproduce across laboratories. We developed an ELISA and multiplex assay to model the cross-linking of Fcγ receptors (FcγR) by Abs, which is required to initiate an ADCC response. Our FcγR dimer ELISA readily detected Abs in samples from two separate cohorts of the partially efficacious Thai RV144 HIV vaccine efficacy trial. The FcγR dimer–binding Abs induced by the RV144 regimen correlated well with a functional measure of ADCC as well as IgG subclasses. The high-throughput multiplex assay allowed us to simultaneously measure FcγR dimer–binding Abs to 32 different HIV Ags, providing a measure of the breadth of FcγR-binding Abs induced by the RV144 trial. FcγR-binding Abs specific to V regions 1 and 2 were strongly associated with increased breadth of recognition of different Env proteins, suggesting anti–V regions 1 and 2 Abs may be a marker of ADCC breadth. This FcγR dimer provides an important tool for the further analysis and refinement of ADCC-inducing HIV and other antiviral vaccine regimens. ***The Journal of Immunology*****, 2017, 199: 816–826.**

Human immunodeficiency virus type 1 (HIV-1) continues to be a significant global health burden (1). A safe and effective vaccine is urgently needed. Historically, a crucial step in the development of effective vaccines has been the development of simple, well-validated assays that correlate with protective immunity (2). This has allowed rigorous step-wise improvements of vaccines needed to reach goals of high efficacy. In the case of HIV-1, one trial, the RV144 HIV-1 vaccine trial in Thailand, generated a modest efficacy of 31.2% (3). The regimen consisted of a recombinant Canarypox viral-vector prime ALVAC-HIV, containing HIV-1 protein vectors including subtype B Gag (LAI) and subtype A/E envelope (92TH023) along with gp120 subunit vaccine AIDSVAX, containing envelope protein subtypes B (MN) and A/E (A244) (3). IgG Abs generated against V regions 1 and 2 (V1V2) of Env correlated with a reduced incidence of HIV-1 acquisition in vaccine recipients (4, 5). Subsequent analyses point toward non-neutralizing Abs with Fc-mediated functions playing a role in the anti-Env Ab immunity induced by this trial (6, 7).

A potential role for Ab-dependent cellular cytotoxicity (ADCC) Abs in the limited success of the RV144 trial is consistent with a growing body of literature on the role of ADCC in control of viremia and disease progression in HIV-infected subjects (8–10). The ADCC response bridges the innate and adaptive arms of the immune system, where Abs bind via their F_{ab} region to viral epitopes and their Fc portion binds to, and aggregates Fcγ receptors (FcγR) on innate effector cells such as NK cells, monocytes and macrophages, and neutrophils. The aggregation of FcγR initiates a signaling cascade within the cell (11, 12), leading to the activation of effector cells (13–16). FcγRs found on different immune cells initiate distinct antiviral functions. FcγRIIIa is primarily found on NK cells and its cross-linking is crucial for activation of NK cell–mediated ADCC, along with the secretion of cytokines and chemokines (13). FcγRIIa is present on macrophages and neutrophils, which induce Ab-dependent cellular phagocytosis (ADCP) of immune complexes (17). ADCP has correlated with protection against SIV infection in prime-boost vaccine macaque studies (18). The strength of IgG interaction with the FcγR is also influenced by genetic polymorphisms (19). Functionally important allelic variants of FcγRIIIa include higher affinity FcγRIIIa-V158 and lower affinity FcγRIIIa-F158, and

*Department of Microbiology and Immunology, Peter Doherty Institute for Infection and Immunity, The University of Melbourne, Parkville, Melbourne, Victoria 3000, Australia; [†]Centre for Biomedical Research, Burnet Institute, Melbourne, Victoria 3004, Australia; [‡]Department of Immunology, Monash University Central Clinical School, Melbourne, Victoria 3004, Australia; [§]Department of Pathology, The University of Melbourne, Parkville, Melbourne, Victoria 3010, Australia; [¶]Melbourne Sexual Health Centre, Infectious Diseases Department, Alfred Health, Monash University Central Clinical School, Melbourne, Victoria 3053, Australia; and [‖]Australian Research Council Centre of Excellence in Convergent Bio-Nano Science and Technology, The University of Melbourne, Parkville, Melbourne, Victoria 3010, Australia

[1]A.W.C. and S.J.K. contributed equally to this work.

ORCIDs: 0000-0002-5845-3307 (M.R.M.); 0000-0002-4108-375X (B.D.W.); 0000-0002-0360-7890 (P.M.H.); 0000-0002-8539-4891 (S.J.K.).

Received for publication December 27, 2016. Accepted for publication May 17, 2017.

This work was supported by Australian National Health and Medical Research Council Awards. Institutional support was provided by the RV144 study and analyses from the Armed Forces Research Institute of Medical Sciences, the Military HIV Research Program, the Thai Ministry of Public Health, Mahidol University, the Royal Thai Army, and BioPHICS Centre of Excellence for Biomedical and Public Health Informatics.

The views expressed are those of the authors and should not be construed to represent the positions of the U.S. Army or Department of Defense.

Address correspondence and reprint requests to Prof. Stephen J. Kent and Dr. Amy W. Chung, Department of Microbiology and Immunology, Peter Doherty Institute for Infection and Immunity, The University of Melbourne, 792 Elizabeth Street, Parkville, Melbourne, VIC 3000, Australia. E-mail addresses: skent@unimelb.edu.au (S.J.K.) and awchung@unimelb.edu.au (A.W.C.)

The online version of this article contains supplemental material.

Abbreviations used in this article: ADCC, Ab-dependent cellular cytotoxicity; ADCP, Ab-dependent cellular phagocytosis; FcγR, Fcγ receptor; HIV-1, HIV type 1; MFI, median fluorescence intensity; RFADCC, rapid-fluorimetric ADCC assay; V1V2, V regions 1 and 2.

FcγRIIa consists of isoforms such as FcγRIIa-H131 and FcγRIIa-R131 (19), which have differing affinities and specificity for IgG2. The IgG1 and IgG3 subclasses that bind most avidly to FcγRIIIa are linked to enhanced efficacy in the RV144 trial (7, 8).

There is a growing interest in the role of ADCC in the efficacy of HIV vaccines. Additional RV144-like HIV vaccine efficacy trials have recently been initiated (20). The substantial investment in these efficacy trials emphasizes the significant need for robust and high-throughput standardized assays to measure ADCC immunity. Cell-based ADCC assays can be difficult to standardize or reproduce precisely across laboratories (21, 22), more so than neutralizing Ab assays where the field has invested significantly in standardized assays (23). Current cell-based ADCC assays typically measure the expression of cytokines and lytic proteins or the killing capacity of NK cells (8, 24–26). Such Ab-mediated assays include the rapid-fluorimetric ADCC assay (RFADCC) (27), viral inhibition assays (28, 29), lactate dehydrogenase release killing assay (30), granzyme delivery assays (31), and NK cell–activation assays measuring IFN-γ and/or CD107a (13). Substantial variation across human effector cell donors influences the readouts of these assays, adding to issues around variability, standardization, and reproducibility across laboratories (32). One aspect that has limited study for HIV-specific ADCC in the vaccine field is the breadth of the response across multiple strains (33). This is clearly important in terms of recognizing different viral strains, and potentially for protecting against a range of field isolates, but is relatively cumbersome to study with standard ADCC assays.

In recent years, several groups have begun to study soluble FcγRs, either as monomers or tetramerized monomers, to use as ELISA or multiplex-based reagents to study the binding of Env protein–Ab complexes (34–36). This greatly simplifies the analysis of FcγR-binding Abs in HIV studies. However, we surmised that an improved reflection of the process of innate cell activation through FcγR binding would be facilitated by developing FcγR dimers linked by the receptor membrane proximal stalk. To this end, we recently developed and studied a novel ELISA-based assay to detect the binding of influenza hemagglutinin Ag-specific Abs to the dimerized ectodomains of two FcγRs joined by a membrane proximal stalk (37). This FcγR dimer ELISA assay was effective in identifying IgG FcγRIIa-mediated functions against influenza proteins (30, 38) and in this study we used this probe to investigate plasma samples from the RV144 HIV-1 vaccine trial, including developing a new multiplex assay using fluorescent beads coated with a broad array of 32 different HIV-1 Env Ags. This allowed a novel in-depth study of the breadth of FcγR-binding Abs induced by the RV144 trial. Taken together, our results both further characterize the immunity of the RV144 trial and suggest this novel FcγR dimer ELISA assay will prove useful in analyses of future HIV vaccine trials.

Materials and Methods

Clinical trial serum samples

RV144 phase III clinical trial (3) plasma samples were kindly provided by the U.S. Military HIV Research Program in separate shipments of 45 and 100 samples. We studied samples from week 26 (2 wk post vaccination) RV144 vaccine recipients (n = 30; n = 80 for the two shipments), week 0 RV144 vaccine recipients (n = 10; n = 10 for the two shipments), and week 26 RV144 placebo subjects (n = 5; n = 10 for the two shipments). Healthy uninfected subjects (n = 5) also gave blood as control samples. The relevant human research ethics committees approved all studies.

HIV-1 Ags

HIV-1_{A244}gp120 (catalog #12569) and HIV-1_{MN}gp120 (catalog #12570) Env Ags were specifically matched to the same subtypes included in the RV144 vaccine regimen. Gag antigenicity was tested using p24 protein subtype B (IIIB) (catalog #1202, all generously provided by the National Institutes of Health AIDS Reagent Program). For breadth studies 32 different Env clade proteins and scaffolds were also tested.

ELISA-based FcγRIIIa and FcγRIIa dimer-binding assay

Following the binding of IgG Abs to Ag epitopes, IgGs cross-link and their Fc-regions bind to FcγR causing receptor aggregate ion. A novel ELISA-based IgG assay using a soluble FcγR dimer recapitulates this process in vitro as previously described (37, 38). Briefly, recombinant soluble homodimers of either FcγRIIIa or FcγRIIa were constructed as single, biotin-tagged polypeptides (37). This FcγR dimer ELISA assay was used in this study to quantify the IgG specific to HIV-1 proteins binding FcγRIIIa or FcγRIIa dimers in close proximity. HIV-1 Ags at 50 ng per well diluted in PBS as well as no Ag control for each sample were coated on 96-well flat-bottom MaxiSorp plates (Nalgene Nunc, Rochester, NY). HIVIG (#3957; National Institutes of Health AIDS Reagent) at 5 μg/ml was coated on the plate at the same time to normalize FcγR activity across different plates. Following overnight incubation at 4°C, the ELISA plates were washed with PBS containing 0.05% Tween20 (LabChem) and blocked for 1 h at 37°C with 140 μl PBS containing 1 mM EDTA (#AM9260G; Ambion, Thermo Fisher Scientific) and 1% BSA (Sigma-Aldrich) (PBSE + 1% BSA). Following plate washing, heat-inactivated RV144 (56°C for 45 min) serum was added at 1:10 dilution in PBSE + 1% BSA [determined using endpoint titration analyses using half-log dilutions of RV144 wk 26 plasma (n = 6) against each Ag]. After incubation and washing, 0.1 μg/ml purified FcγIIIa-V158 dimer-biotin or 0.2 μg/ml FcγRIIa-H131 dimer-biotin diluted in PBSE + 1% BSA was added to every well of the plate. Following incubation and wash, HRP-conjugated streptavidin (#21130; Thermo Fisher Scientific) was added in 1:10,000 dilution with PBSE + 1% BSA. After incubation and washing, color was developed using 3,3′5,5′-tetramethylbenzidine (Sigma-Aldrich) followed by 1 M HCl stop solution. Absorbance at 450 nm wavelength was recorded as OD. No Ag values were deducted from each Ag sample and then normalized to 5 μg/ml HIVIG. A positive signal was defined as an OD higher than mean + 3 × SD of OD obtained using sera from five HIV-1 negative donors against each Ag tested.

ELISA-based FcγRIIa-H131 monomer, tetramerized monomer, and tetramerized dimer–binding assay

To compare the effect of FcγR valency, the activity of the ELISA using dimeric rsFcγRIIa-H131 was compared with ELISA using a monomer, biotin-streptavidin tetramer of monomers, or biotin-streptavidin tetramer of dimers. The receptor forms were produced as above (37). The ELISA was performed as above with separate wells, and after the plasma incubation and washes, 0.2 μg/ml FcγRIIa-H131 monomer instead is added to the well at that same step. Separately, 0.2 μg/ml tetramerized FcγRIIa-H131 dimer and 0.2 μg/ml tetramerized FcγRIIa-H131 monomer are constructed by adding HRP-streptavidin with the biotinylated FcγRIIa-H131 dimer or FcγRIIa-H131 monomer in the same step, incubated together for 1 h and followed with the remaining dimer-binding protocol after HRP-streptavidin is normally added.

RFADCC assay

To compare the FcγR dimer assays with a standard cellular readout of Ab-mediated Fc function, the RFADCC assay was employed in this study to measure total CFSE dye loss from killed CEM target cells as previously described (27). The mechanism behind the $CFSE^-$ CEM target cells was further examined by measuring the uptake of PKH26 membrane dye target cells by CD14 positive monocytes as previously described (39) along with identifying nonmonocytic CD14 negative $PKH26^+CFSE^-$ killed CEM cells. The gating strategy is described in Supplemental Fig. 1. In brief, 10^6 CEM.NKr-CCR5 cells in RF10 medium were pulsed with 30 μg/ml HIV-1 A244gp120 protein or remained uncoated for 1 h at room temperature. CEM.NKr-CCR5 cells were then labeled with 7.5×10^{-7} M PKH26 membrane dye (Sigma-Aldrich) solution for 4 min then stopped with 400 μl FCS. Cells were washed twice with PBS and then stained with 5×10^{-8} M CFSE (Sigma-Aldrich) as an intracellular dye for 3 min, then stopped with 400 μl FCS. Following two washes with PBS and one with RF10, 2×10^4 $PKH26^+/CFSE^+$ stained CEM.NKr-CCR5 cells were incubated with 2 μl plasma (1:100 dilution) for 30 min at 37°C followed by the addition of 2×10^5 PBMCs (10:1 effector: target ratio) and a 4 h incubation at 37°C. Following incubation, cells were stained with anti-human CD14-APC.H7 and anti-human CD3-PerCP (BD Biosciences), washed, and fixed with 10% formaldehyde. The cells were acquired with a FACS BD LSR Fortessa cytometer and analyzed with FlowJo software 10.1v7. HIVIG was used as a positive control and acted to normalize data across assays and replicates. To study more directly the effect of NK cells in the RFADCC assay, NK cells were purified from healthy

donor blood using NK cell rosette sep kit (Stemcell) according to the manufacturer's instructions. Purified cells were stained as CD3-PerCP negative, CD56-PE, and CD16-AlexaFluor700 positive (BD Biosciences) to confirm purity. A modified NK cell–mediated RFADCC assay was performed using the same conditions as previously described (6).

Multiplex array to study cross-clade reactivity of ADCC Abs

To study the breadth and potency of the FcγR-binding Abs in more detail, we developed a customized multiplex assay. This assay has the capacity to simultaneously detect Ab recognition of a panel of 32 different HIV Ags in a single well, minimizing the amount of vaccine plasma sample used along with the assay time required to repeat multiple ELISAs. A diverse panel of 32 HIV proteins was covalently conjugated to individual microspheres with different fluorescences as previously described (40). The protein-conjugated beads (minimum of 500 of each individual coated bead set per well) were incubated with RV144 plasma from week 0, week 26, placebo, and HIV-1 negative at 1:100 plasma dilution (total volume 1 μl plasma: 99 μl PBS + beads), overnight at 4˚C on a plate shaker. The beads were washed using a Bio-Rad magnetic plate-washer (BioPlex Pro wash station) and incubated for 2 h on a plate shaker at room temperature, then subsequently with PE-conjugated anti-human Abs that either recognized total IgG, IgG1, IgG2, IgG3, or IgG4 (Southern Biotech) (40) or dimeric biotinylated FcγR (human FcγRIIa-H167, FcγRIIIa-V158) (37) followed by streptavidin-PE (an additional 1 h incubation). HIVIG was used to normalize data across multiple replicates, whereas VRC01 and PGT121 mAb was used to normalize Env protein bead coating of the same strains, allowing for comparisons of gp120 and gp140 of the same Env strain. A Bio-Plex reader (Bio-Plex MAGPIX, Bio-Plex Manager 5.0, Bio-Rad) was used to detect the microspheres and binding of PE fluorescence was measured to calculate a median fluorescence intensity (MFI). Background signal, defined as the average MFI observed for each microsphere set when incubated with the PE-conjugated detection reagent in the absence of Ab sample, was subtracted from the MFI for each sample. To examine FcγR dimer binding cross-clade breadth, two different analysis approaches were used to account for the difficulty in normalizing across diverse HIV protein Ags. Although broadly neutralizing mAb (VRC01 and PGT121) that bind to all clades were available to standardize differences between gp120 and gp140 protein of the same strain, they have variable binding potency across clades, due to the high variability in structures of Env proteins. Thus, the first analysis involved examining breadth in relation to the maximal possible FcγR binding observed across the entire bead array to all RV144 samples. All FcγR binding to remaining HIV Ags were then scored relative to 50% of this maximum potential binding. To validate the findings, we used a second analytical approach of first standardizing all data by calculating respective z-scores, then identifying FcγR binding responses in the top 50% of each respective HIV Ag separately.

Statistical analyses

Statistical analyses were completed using Prism GraphPad version 7.0 (GraphPad Software, San Diego, CA). Once data were normalized to HIVIG, Mann–Whitney nonparametric U tests were used to compare week 0 and week 26 results for each Ag; Bonferroni multiple comparison correction was completed and the significance level adjusted accordingly. Nonparametric Spearman correlation analyses were used to test for correlations. The open software Morpheus heatmap program (https://software.broadinstitute.org/morpheus/) was used to generate heatmaps. A p value <0.05 indicates the level of significance, unless otherwise stated.

Results

FcγR dimer–binding Abs induced by the RV144 vaccine regimen

Following the interest in ADCC responses found in RV144 vaccinees and our previous studies in anti-influenza ADCC (37, 38), we applied a novel FcγR dimer–based ELISA assay to a series of plasma samples from the R144 trial. We first studied the FcγR dimer ELISA assay using purified HIV-1 Env Ags (A244gp120 and MNgp120, the proteins used as boosts in the RV144 trial). Sera from the RV144 vaccine trial participants were then added, followed by addition of FcγR dimer constructs. These bind the IgG-opsonized Env only if the Fcs of pairs of Abs are able to simultaneously bind the two ligand-binding domains of the dimeric FcγR. We studied samples using the higher-affinity FcγRIIIa-V158 dimer, a low-affinity FcγRIIIa-F158 dimer, and an FcγRIIa-H131 dimer (Fig. 1A, 1C). The assay readily detected Env-specific FcγRIIIa-V158 and FcγRIIa-H131 dimer–binding Abs in RV144 vaccine recipients across 30 vaccinees. Negligible FcγR dimer–binding was detected in the RV144 placebo, baseline (week 0), or HIV-1 negative samples. The greatest FcγR dimer–binding Ab responses were detected against the subtype AE A244gp120 present in the boosting protein vaccine (Fig. 1A, 1B), followed by those specific for the subtype B MNgp120 and only weak recognition of Gag p24, consistent with the Ags present in the prime-boost vaccines. The strongest responses were detected with the high-affinity FcγRIIIa-V158 isoform and only weak responses were detected with the low-affinity FcγRIIIa-F158 isoform. To validate these responses, a larger cohort of 80 RV144 vaccinees was tested, again with significant vaccine-specific responses detected (Fig. 1D). Identical experiments on the initial cohort were repeated under the same conditions 7 mo later and significantly correlated ($p = 0.0001$). Across these two cohorts the median and SD of FcγRIIIa-V158 dimer–binding responses post vaccination were almost identical between the initial cohort of 30 subjects studied (0.748 ± 0.250 Fig. 1A, left panel) compared with the validation cohort of 80 subjects studied (0.752 ± 0.269, Fig. 1D).

Comparison between RV144 generated Env-specific Abs binding FcγR dimer, monomer, tetramerized monomer, and tetramerized dimer reagents

Prior studies have used FcγR monomer and tetramer reagents to analyze FcγR-binding Abs (35); however, our previous influenza studies suggest that the use of dimeric FcγR dimer reagent is both more physiologically relevant and sensitive in detecting FcγR-binding Abs (37). With an identical ELISA protocol as used for each FcγR isoform, we compared similar reagents currently being used in the field to the biologically relevant FcγR dimer construct. Monomeric forms of FcγRIIa-H131 generated higher levels of background and had comparatively lower levels of recognition (median 0.122) (Fig. 2). In comparison, FcγR dimer produced lower background responses in controls and a broader dynamic range (median 0.80) than the other FcγR reagents (Fig. 2).

RFADCC analyses of RV144 plasma samples

Our previous work in influenza suggested that the FcγR dimer ELISA correlated well with measures of functional ADCC using cell-based assays (37, 38). Using the functional RFADCC assay commonly used in the HIV vaccine field, we evaluated whether RV144 induced Env-specific Abs capable of eliciting functional activities. The RFADCC assay uses whole PBMC as effectors and can be analyzed in three ways that may reflect mechanistic differences in Ab subclasses and/or Fc-mediated functions. The standard analysis of the RFADCC assay (gating is shown in Supplemental Fig. 1C) measures total PBMC lysis of target cells via the loss of target cell intracellular dye CFSE and retention of membrane surface dye $PKH26^+$; we refer to this as RFADCC killing, and the results across all 30 vaccinees and various controls are shown in Fig. 3A.

However, previous research from our group has shown that a substantial amount of the killing observed in the standard RFADCC analysis is uptake of lysed target cells by $CD14^+$ monocytes (39). We therefore gated on $PKH26^+CFSE^-$ CD3-$CD14^+$ monocytes (gating shown in Supplemental Fig. 3D); referred to as RFADCC monocyte uptake. The results of this analysis across 30 vaccinees and controls are shown in Fig. 3B. However, the monocyte uptake analysis excludes a proportion of PKH^+CFSE^- cells that are not monocytes (19.1% in the example shown in Supplemental Fig. 3D); we term this analysis nonmonocytic killing as it may reflect Fc-mediated killing of target cells by other Fc-receptor bearing cells. The analysis of this population across all 30 vaccinees and controls is shown in Fig. 3C.

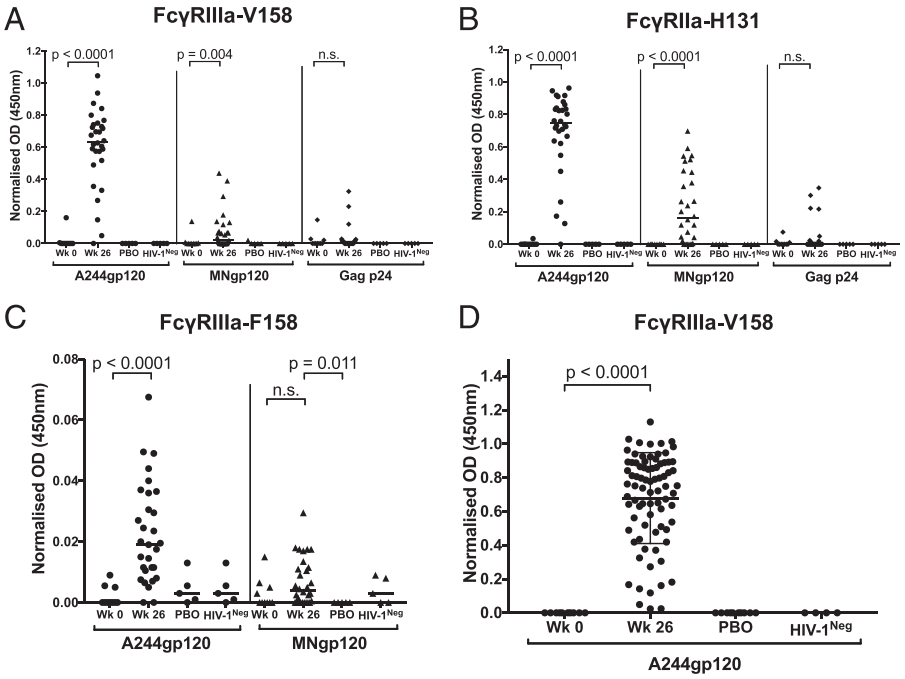

FIGURE 1. FcγRIIIa and FcγRIIa dimer–binding assays. (**A**) FcγRIIIa-V158 binding Ab responses and (**B**) FcγRIIa-H131 binding Ab responses to gp120 strain A/E (A244gp120; left panel), gp120 strain MN (MNgp120; center panel), and Gag p24 (right panel) proteins. Responses are normalized to 5 μg/ml HIVIG. (**C**) FcγRIIIa-F158 low affinity binding Ab responses to A244gp120; MNgp120. (**D**) FcγRIIIa-V158 binding Ab responses to gp120 strain A/E (A244gp120) protein. A validation of the novel dimer-binding assay using a larger cohort. Wk 0 and Wk 26 were compared using Mann–Whitney nonparametric *t* test. $p < 0.05$ was considered significant and lines indicate median. PBO, placebo.

Prevaccination samples showed no positive results using any of the three analyses of the RFADCC assay, and as expected, week 26 vaccinees show positive responses across all three analyses (Fig. 3A–C). To assess whether the FcγRIIIa-V158 and IIa-H131 dimer assays act as a proxy for functional assays, we correlated the dimer assays with analyses of the RFADCC assay. We observed the highest correlation ($r = 0.52$, $p = 0.0031$) between RFADCC nonmonocytic killing and FcγRIIIa-V158 (Fig. 3F, left panel). RFADCC killing also correlated significantly with both FcγR dimers (Fig. 3D) as did RFADCC monocyte uptake with both FcγRIIIa-V158 and FcγRIIa-H131 (Fig. 3E).

Multiple potential effector cells with variable expression profiles of multiple FcγRs are present within PBMCs, which limits the capacity to examine functions mediated through individual FcγRs. To compare the FcγR dimer assays with the functional output of a specific effector population, we purified out NK cells, which only express FcγRIIIa, and conducted a similar NK cell–mediated RFADCC assay measuring CFSE loss from target CEM.NKr.CCR5 cells. We found a strong correlation between FcγRIIIa-V158 dimer–binding and NK RFADCC data ($r = 0.64$, $p = 0.0002$; Fig. 4G, left panel) and a notable correlation between FcγRIIa-H131 and NK RFADCC data ($r = 0.47$, $p = 0.0088$; Fig. 4G, right panel).

Correlations of Env-specific FcγR dimer–binding Abs and RFADCC responses with IgG subclasses

IgG subclasses have been linked to both ADCC responses and protection in the RV144 trial (6, 7). We measured Env-specific IgG subclasses 1–4 using a multiplex assay as previously described (40) and analyzed the relationship between FcγR binding, IgG subclasses, and the different effector cell fractions that contribute to RFADCC activity in a heatmap format. In Fig. 4, we display RV144-vaccinated individual responses ($n = 30$) in each assay in a correlation matrix of coefficients that displays *r*-values (Fig. 4A) as well as respective *p* values (Fig. 4B). IgG subclasses (IgG1, IgG2, IgG3, and IgG4) have different affinities and specificities for Fcγ-receptor isoforms FcγRIIIa-V158, FcγRIIa-H131, and

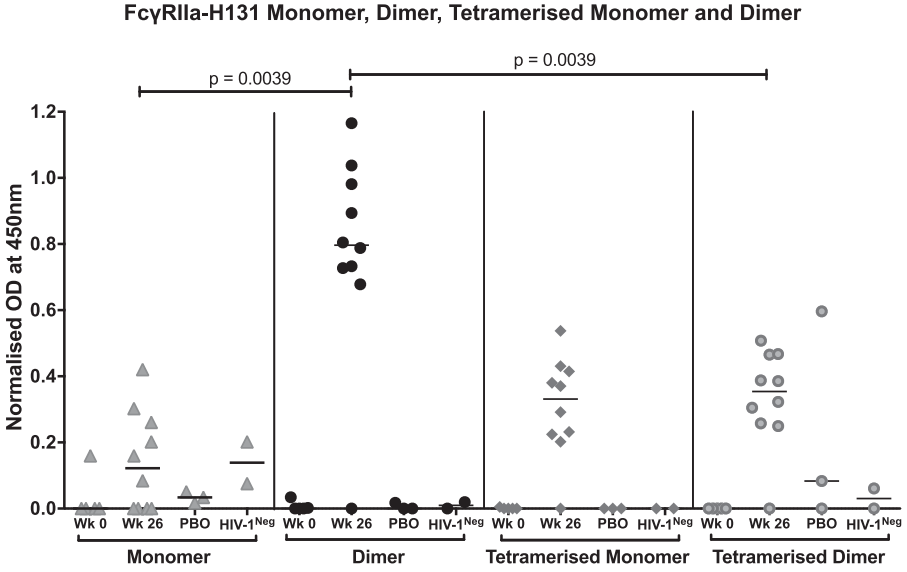

FIGURE 2. FcγRIIa monomer, dimer, tetramerized monomer, and tetramerized dimer–binding ELISA assays with RV144 plasma samples against A244gp120. OD normalized to 5 μg/ml HIVIG. Significance level for all tests set at $p = 0.05$. PBO, placebo.

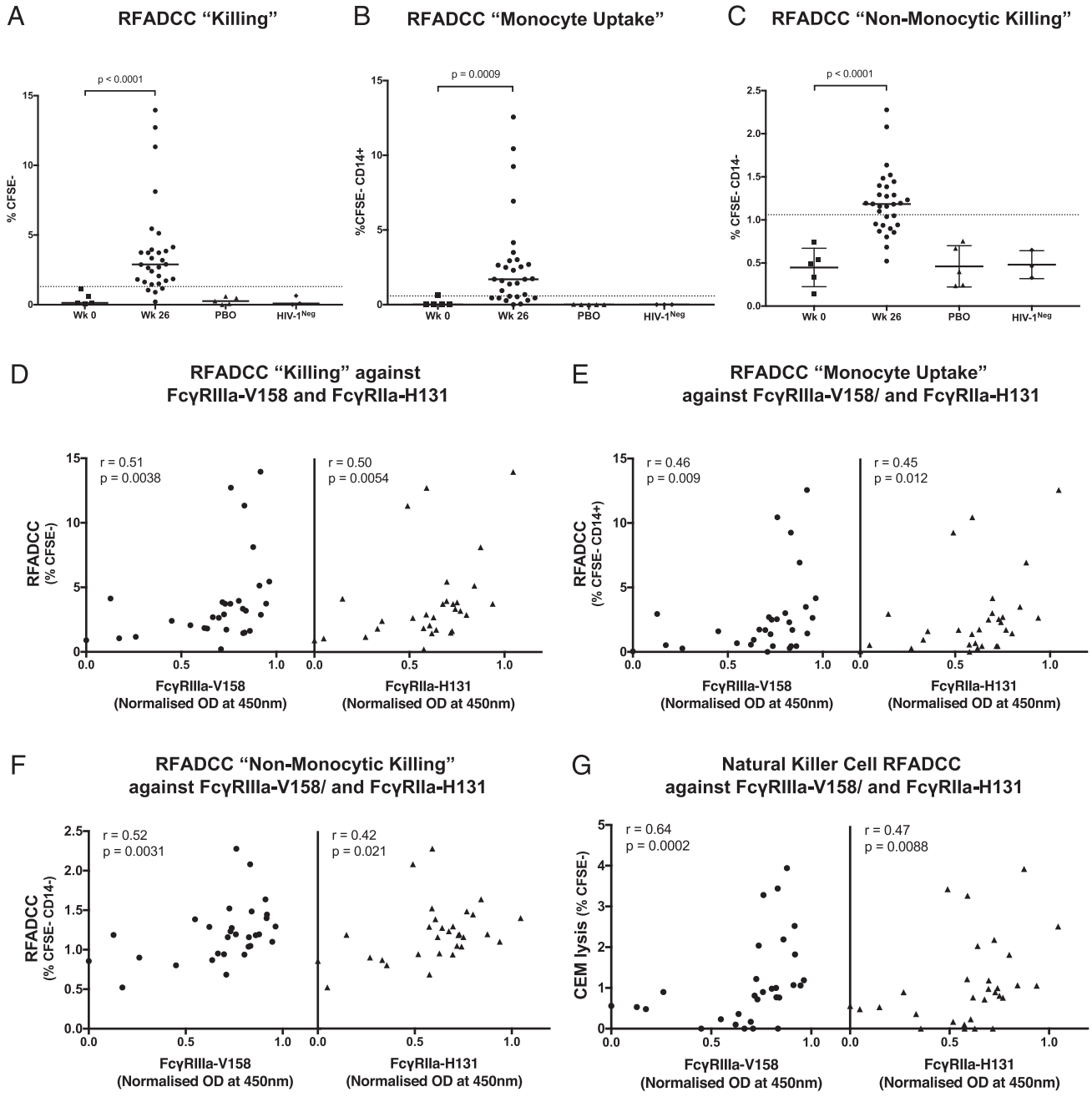

FIGURE 3. RFADCC functional assays and their correlations with dimer-binding assays with A244gp120 protein. (**A**) RFADCC measuring killing via $CFSE^-$ target cells, (**B**) RFADCC measuring CD3-$CD14^+$ monocytes with PKH^+ $CFSE^-$, and (**C**) RFADCC analyzed to measure $CFSE^-$ $CD14^-$ target cells. Dotted lines on *y*-axes represent mean + (3 × SD) of negative controls. Plasma diluted at 1 in 100 against A244gp120 Ag. Mann–Whitney *t* test compared week 0 to week 26. Scatter plot matrix depicting Spearman correlation comparing RFADCC $CFSE^-$ data (**D**), RFADCC $CFSE^-$ $CD14^+$ data (**E**), $CFSE^-$ $CD14^-$ data (**F**), and NK cell RFADCC CEM cell lysis ($CFSE^-$) (**G**) with FcγRIIIa-V158 and FcγRIIa-H131 binding Ab data against A244gp120 Ag. Matched pairs analyses. Significance level for all comparisons was set at $p = 0.05$. PBO, placebo.

FcγRIIIa-F158. The FcγRIIIa-V158 and FcγRIIa-H131 dimer ELISAs correlated most strongly with IgG1 and IgG3, consistent with previous RV144 correlates studies (6, 7). Interestingly, RFADCC monocyte uptake correlated stronger with IgG2 ($r = 0.56$, $p = 0.0014$) and IgG1 ($r = 0.56$, $p = 0.0013$) than IgG3 ($r = 0.3$, $p = 0.1132$), whereas in comparison nonmonocytic killing correlated with IgG1 ($r = 0.69$, $p < 0.0001$) and IgG3 ($r = 0.49$, $p = 0.006$), but not IgG2 ($r = 0.26$, $p = 0.1663$). Nonmonocytic killing correlated strongest with FcγRIIIa-V158 ($r = 0.52$, $p = 0.0031$). This may reflect the different FcγR mechanisms associated with different effector cells because monocytes express both FcγRIIa (which is known to bind to IgG1, IgG2, and IgG3) and FcγRIIIa (preferentially binds IgG1 and IgG3), whereas NK cells express only FcγRIIIa. Negative and low correlations were observed between IgG4 and FcγRIIIa-F158 (Fig. 4A, 4B). Purified NK cell–mediated target cell lysis correlated strongest with FcγRIIIa-V158 and FcγRIIa-H131 ($r = 0.71$, $r = 0.72$; $p < 0.0001$, $p < 0.0001$) with strong correlations also with IgG1 ($r = 0.61$, $p = 0.0003$) and IgG3 ($r = 0.59$, $p = 0.0006$) (Fig. 4A, 4B).

Breadth analyses using a novel multiplexed FcγRIIIa and FcγRIIa dimer ELISA

An ability to generate Fc-functional Abs to multiple HIV strains may be important in providing protection across exposures to diverse HIV strains. The FcγR dimer assay was therefore adapted

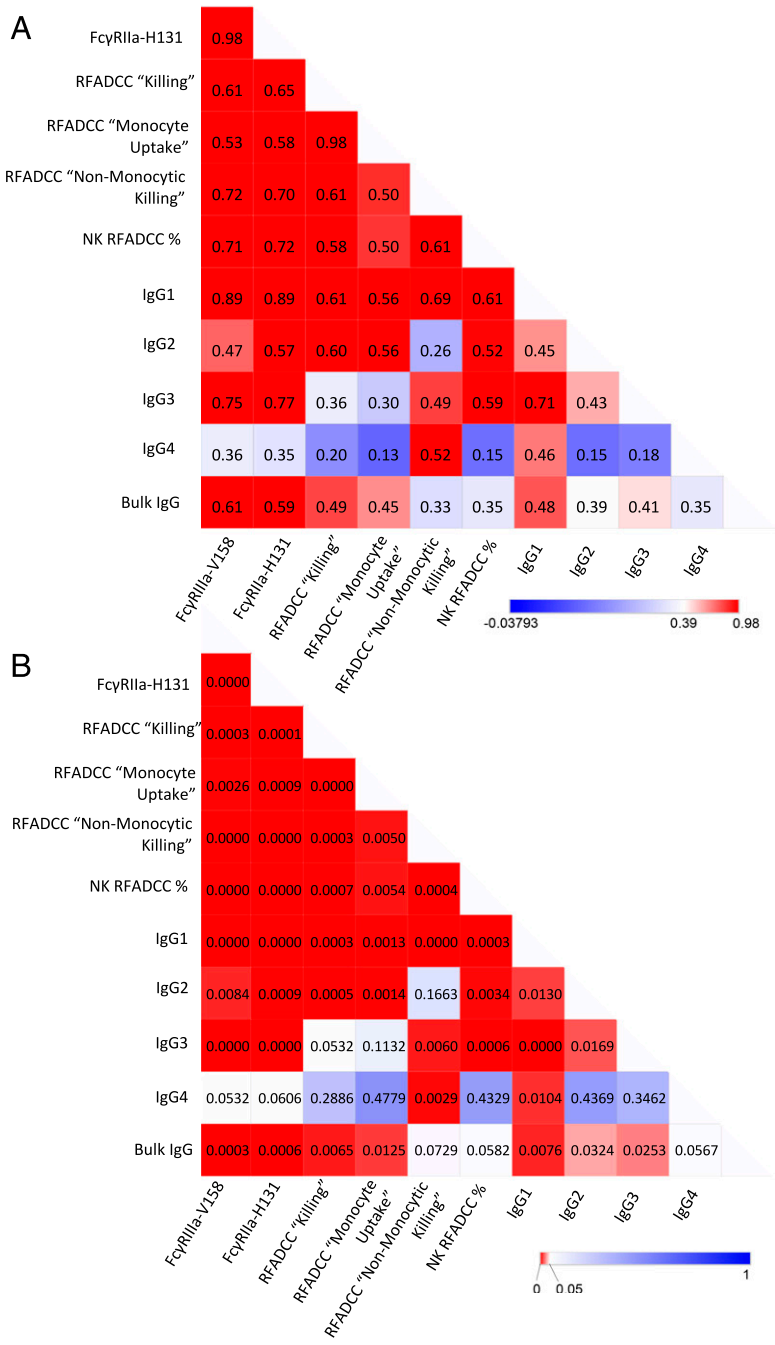

FIGURE 4. Heatmap with correlation matrix. (**A**) Depicts Spearman rank correlation coefficients and top right depicts corresponding *p* values of week 26 RV144 plasma responses to FcγRIIIa-V158, FcγRIIa-H131, and FcγRIIIa-F158 binding as measured by multiplex, RFADCC monocyte data, RFADCC PBMC data, RFADCC NK cell data, and IgG isotype binding to A244gp120. Red (value of 1) represents a stronger correlation coefficient and more significant *p* value. Dark blue represents weaker correlation coefficients and *p* values. (**B**) Depicts respective *p* value for each correlation. Brodmann multiple comparisons correction was not applied for the *p* value, which is set at 0.05 for significance.

to multiplex technology, allowing us to examine cross-clade breadth binding to 32 HIV-1 Env by coating beads with different fluorescence markers for each Env protein. Fig. 5A illustrates primary data from this assay, yielding an MFI for FcγRIIIa-V158 dimer bound to the fluorescent HIV Ag–coated beads opsonized with RV144 vaccinee sera from 80 subjects. Fig. 5B displays the same repeated with FcγRIIa-H131 dimer. A very large dynamic range was apparent (~4 $\log_{10}$) compared with the standard OD values from the simpler ELISA. Fig. 5A illustrates four Env proteins studied (consensus M, two subtype B strains, and one C strain) matched for monomeric gp120 and gp140. As previously described for functional ADCC assays (33), gp140 is less well recognized than gp120 by FcγR dimer–binding Abs in each case, likely reflecting a significant proportion of Fc-functional Abs directed at the gp120 inner domain. Fig. 5C illustrates the differences between FcγRIIIa-V158 and FcγRIIa-H131 for the same four Env gp120 proteins studied above, with significantly greater binding to FcγRIIIa-V158 than FcγRIIa-H131 across all four gp120 proteins shown. All 32 HIV Ags are investigated in this way as shown in Supplemental Fig. 2, with 23 of 32 Ags showing significantly greater binding to FcγRIIIa-V158 compared with FcγRIIa-H131. The exceptions to this were two gp41 proteins (C-TM-CZA119MB and B-HXBc2), which had greater binding to FcγRIIa-H131. Surprisingly, no significant difference in binding between the dimers was found between A/E CM235gp120 and A/E 93TH975gp120, which were included in the RV144 regimen (3).

A full analysis of FcγRIIa and FcγRIIIa dimer binding across the 32 HIV Ags studied is shown as heatmaps. FcγRIIIa-binding Abs specific for each HIV-1 Env protein are presented in Fig. 5D, whereas FcγRIIa-binding Abs are illustrated in Fig. 5E. Unsu-

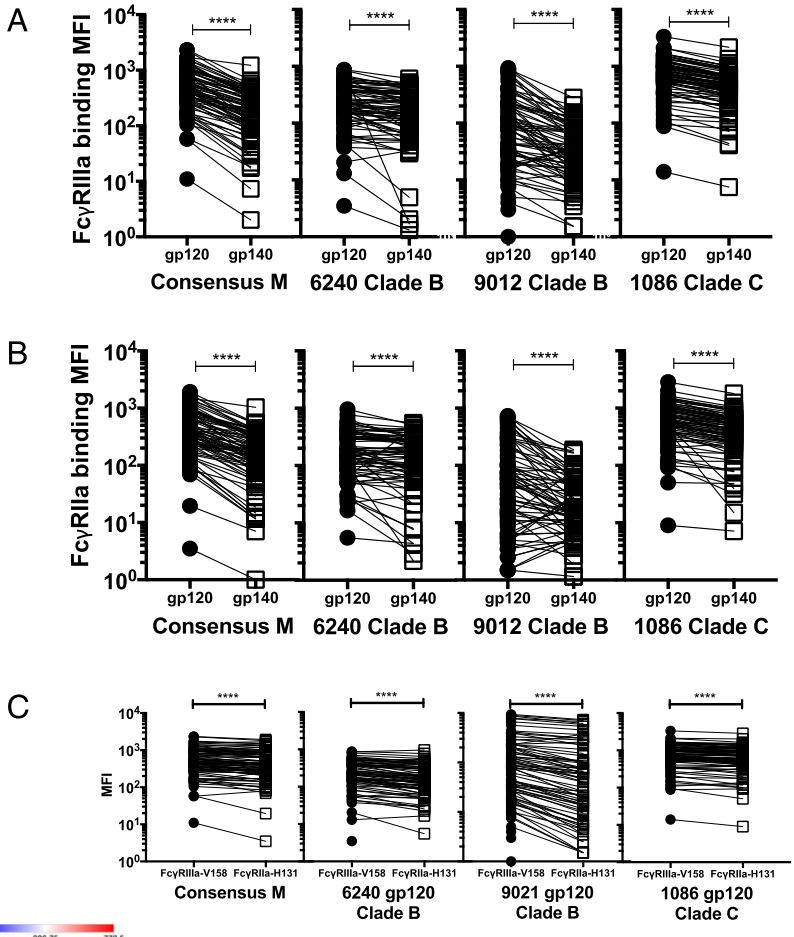

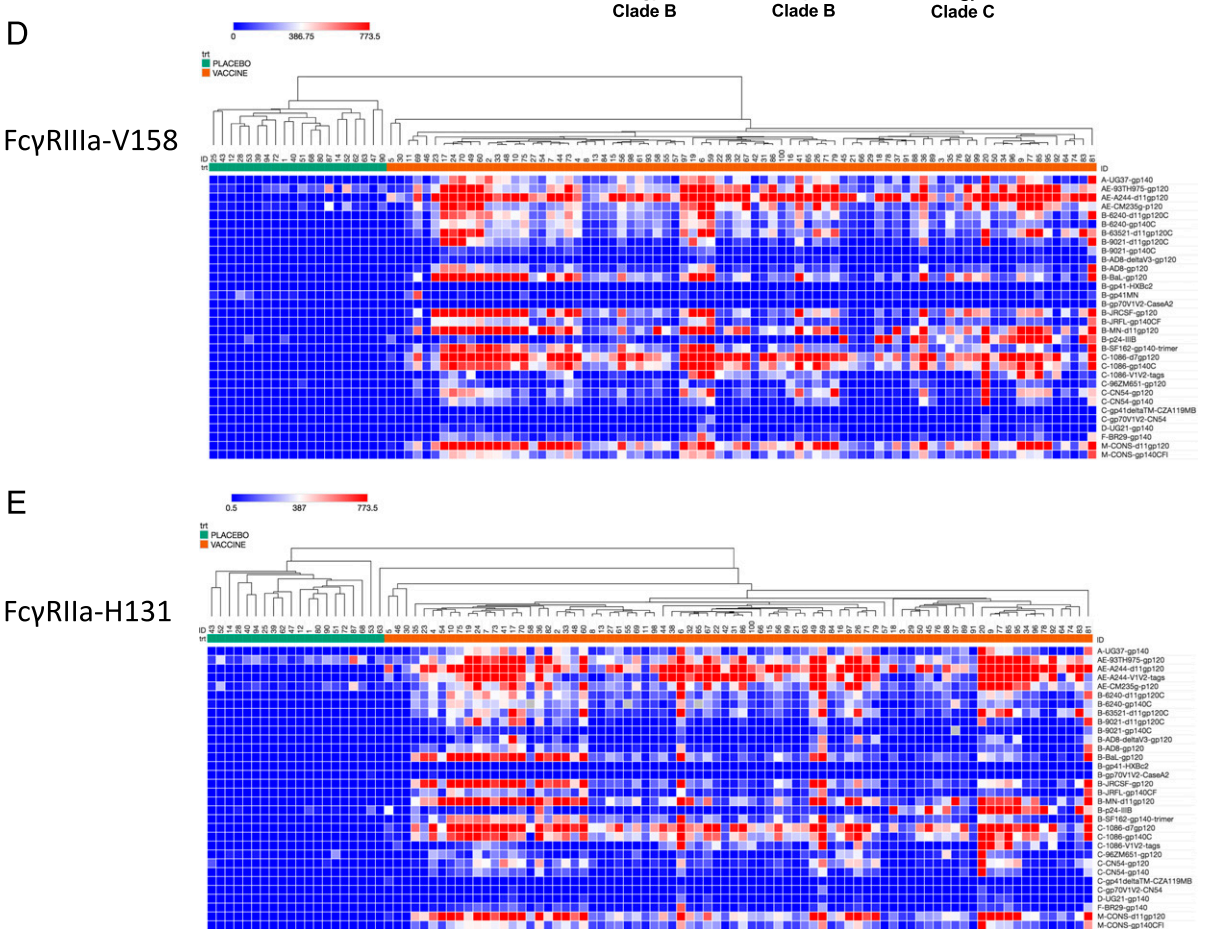

pervised hierarchical clustering of subjects (identified top *x*-axis) naturally separated RV144 vaccinees (orange) from placebos (green). There was greater binding for gp120 proteins compared with gp140, and this trend was seen across both FcγRs (Fig. 5A, 5B). FcγR dimer–binding Abs to Gag p24 were only detected in a subset of vaccinees (consistent with the nonmultiplex assay shown in Fig. 1), and there were virtually no FcγR dimer–binding Abs to gp41 Ags tested. Across all subjects and both FcγRs, there were generally low cross-clade responses to the three Env proteins tested, representative of clades A, D, and F. Unsupervised hierarchical clustering of the 32 Ags was also conducted (Supplemental Fig. 3) and observed notable differences in cluster patterns between FcγRIIIa-V158 (Supplemental Fig. 3A) and FcγRIIa-H131 (Supplemental Fig. 3B), such as distinct separation of clade AE protein binding patterns, were only found for FcγRIIa-H131.

Analysis of V1V2 Ab FcγR binding in relation to breadth

A key finding of initial RV144 correlate analyses was that the strength of anti-V1V2 Abs was an inverse correlate with risk of infection (4), with only subsequent analyses pointing toward nonneutralizing Abs with Fc-mediated functions as another possible correlate (5, 7, 41). Because it is rational that the breadth of recognition of strains by Abs with Fc-mediated functions would be an important aspect of robust immunity, we studied the relationship between anti-V1V2 FcγR dimer–binding Abs (using the vaccine A244 strain) and the overall breadth of FcγR-binding Abs against the other 31 HIV proteins studied. We ranked the RV144 sera samples by strength of anti-V1V2 FcγR dimer binding, with the top row in the heatmaps Fig. 6A and 6B for FcγRIIa and IIIa dimer binding, respectively, illustrating this, and hierarchically clustered the HIV Ags (*y*-axis). The heatmaps illustrate that subjects with stronger anti-A244 V1V2 FcγR dimer binding 1) have stronger FcγR dimer binding to other HIV Ags (i.e., more red on the left side of the maps aligning with stronger anti-V1V2 A244 FcγR dimer); 2) cluster closest with anti-V1V2 FcγR dimer binding to other strains (C-1086 and CN54) and to AE Env gp120 strains A244, 93TH975 and CM235 (i.e., proteins included in vaccine regimen); with 3) the greatest difference was to FcγR dimer binding to gp41 or p24 Abs. Of interest, A244 V1V2 FcγR dimer–binding responders, especially for FcγRIIIa, more closely clustered with clade C Env proteins than clade B.

The association of stronger anti-A244 V1V2 FcγR dimer binding with stronger FcγR dimer binding to other Env Ags suggested by the heatmaps was curious, and we explored it further. To this end, we aimed to define cut-off responses to identify positive or negative FcγR dimer–binding responses for each Env protein. To best evaluate how to analyze these unique and novel data sets we applied two different approaches. The first was to apply a universal positive FcγR dimer–binding threshold determined by examining responses across all RV144 samples and HIV Ags to identify the maximal possible FcγR dimer response to the dataset, then categorize responses as above or below 50% of this maximal FcγR response. In this more stringent cut-off analysis, the overall breadth was found to be low (FcγRIIa: median = 1, range 0–16 recognition of strains, all samples Fig. 6C; FcγRIIIa: median = 2, range 0–16, all samples of Fig. 6D). In the second approach, we standardized all the different HIV Ags with each other and identified a positive relative FcγR response as subjects that fell in the top 50% of each respective Ag. This is a less stringent definition as it creates the assumption that all Ags induced positive FcγR responses. In this analysis, we observed slightly higher breadth, although still a relatively low median, and a much larger range was observed across samples (FcγRIIa: median = 6, range 0–31, all samples Fig. 6E; FcγRIIIa: median = 6, range 0–30, all samples Fig. 6F).

Next, we divided anti-A244 V1V2 FcγR dimer binding into tertiles and studied the breadth of overall Env FcγR dimer binding across the three tertiles (shown in right three columns of Fig. 6C–F). In both types of breadth analyses we observed that higher V1V2 FcγR dimer binding is significantly associated with increased overall breadth. This difference in breadth recognition was strongest when examining the different gp120 proteins, whereas weaker but still significantly higher breadth was observed when examining responses to the different gp140 proteins, and confirmed using both analytical approaches (Supplemental Fig. 4).

Discussion

FcγR binding Abs play an important role in the protection and control of HIV-1 infection (4). Despite the intense interest in ADCC Abs in the HIV vaccine field, there is little consensus on the most appropriate assays to study ADCC. In part this reflects the technical challenges of cell-based ADCC assays and their reproducibility across laboratories (21, 22). Recent studies have used soluble FcγR monomers and tetramers to study these Abs (34, 36). Our recent experience in studying influenza-specific ADCC suggested the FcγR dimer is a very useful reagent to study ADCC Abs (37, 38). In this study we examined 110 RV144 vaccine plasma samples across two sets of samples to opsonize diverse HIV-1 proteins, and measured FcγR binding using novel dimeric FcγR proteins. These dimeric FcγRs readily detected responses induced by the RV144 regimen, and were more sensitive than the equivalent proteins formatted as FcγR monomer or tetramer assays, and correlated with functional ADCC assays and particular IgG subclasses. The nature of the FcγR dimer meant that it was readily adapted to a high-throughput multiplex format to illustrate the breadth of FcγR-binding Ab responses induced by the RV144 trial to a range of 32 Ags across seven different HIV-1 clades. We propose that this assay will prove useful in characterizing the immunogenicity of future HIV vaccine trials and help enable incremental improvements to HIV vaccine efficacy.

The utility of dimeric FcγR binding is determined by its capacity to act as a proxy for cell-based FcγR functional Ab assays. Indeed, significant correlations were found between the FcγR binding and RFADCC assays, reaffirming the biological relevance of the novel dimeric FcγR assays in the setting of HIV immunity. Gp120-specific IgG1 and IgG3 both correlated with FcγRIIIa-V158 binding and importantly with RFADCC killing. Correlations of RFADCC nonmonocytic killing and isolated NK cells with both FcγRIIIa-V158 and IgG1/3 reaffirms previous studies showing IgG1 and IgG3 primarily initiating NK cell mediated ADCC protection in RV144 vaccine recipients (6, 7).

Interestingly, the correlations between RFADCC monocyte uptake with IgG2 and FcγRIIa-H131 dimer are indicative of an

FIGURE 5. RV144 FcγRIIIa-V158 and FcγRIIa-H131 Ab binding protein breadth analyses using multiplex beads. Illustration of enhanced recognition of gp120 compared with gp140 specific binding of the same envelope strains to (**A**) FcγRIIIa-V158 and (**B**) FcγRIIa-H131 dimers. (**C**) Illustration of $****p < 0.0001$ measured by Wilcoxon matched pairs signed rank test. Heatmap showing hierarchical clustering of RV144 vaccine (orange) and placebo (green) samples along the top *x*-axis by (**D**) FcγRIIIa-V158 and (**E**) FcγRIIa-H131 dimer recognition to a range of ENV proteins and scaffolds as measured by multiplex assay. ENV proteins are listed on right-hand *y*-axis; grouped alphabetically in clades. The same scaled legend is applied to both heatmaps. Red indicates greater binding whereas blue represents lower binding.

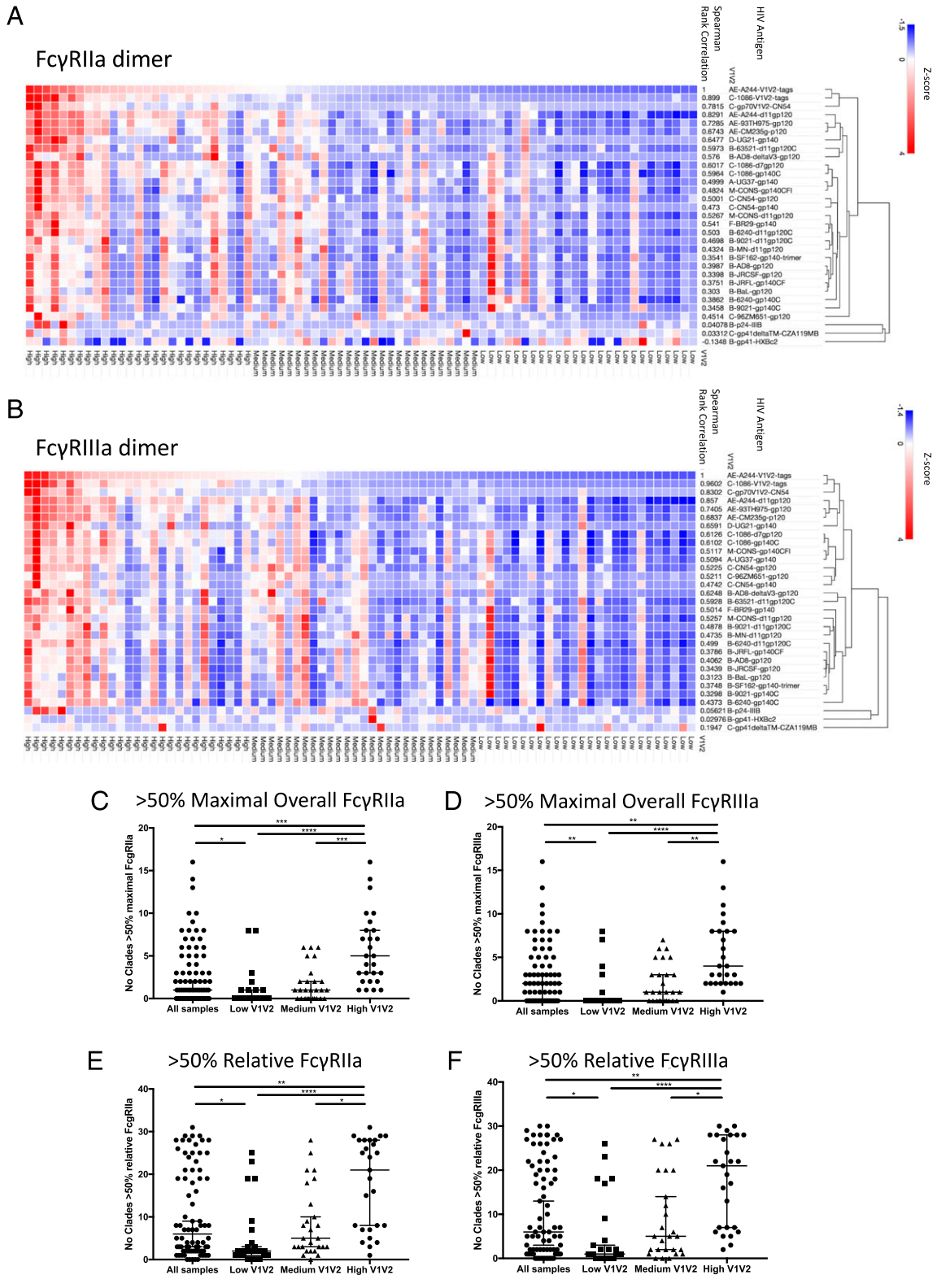

FIGURE 6. Stronger V1V2 specific Ab FcγR binding is associated with enhanced breadth. RV144 FcγRIIa-H131 (**A**) and FcγRIIIa-V158 (**B**) Ab binding responses were standardized by *z*-score and ranked according to V1V2 specific Ab FcγR binding (highest to lowest, left to right). Nearest neighbor comparison with V1V2 Ab FcγR binding for each HIV Ag was also determined (Spearman rank correlation to V1V2 presented on inner right hand side *y*-axis). Maximal FcγRIIa (**C**) and FcγRIIIa (**E**) binding was determined by comparing all HIV Ags and identifying the strongest FcγR Ag (A244gp120 for both FcγRs). Thus >50% maximal was determined by identifying which subjects had FcγR above 50% of the identified maximal response for each Ag. Samples were separated into those that had low, medium, and high V1V2 responses (V1V2 responses separated into tertiles). Relative FcγRIIa (**D**) and FcγRIIIa (**F**) binding was determined by identifying individually for each HIV Ag which subjects had FcγR >50% of the relative maximum binding response for that specific Ag.

alternative mechanism of activation and ADCC lysis of target cells as suggested previously (39). Thus, use of particular FcγR isoforms in the dimer assays is critical for evaluating the full capacity of Ab response to mediate innate immune mechanisms via the varied FcγR expression profiles of different innate immune cells.

Although the cross-clade neutralization reactivity of RV144-induced Abs has been previously investigated, limited ADCC breadth studies have been conducted on RV144 samples, primarily on isolated mAb (41, 42). To date, largely due to costs and labor associated with cell-based ADCC assays, ADCC breadth profiling of RV144 vaccinated individuals has not yet been investigated in detail. Because a goal of HIV vaccines is to provide broad coverage across as many strains as possible, simple methods to characterize the breadth of vaccine-induced FcγR-binding Abs are needed. By adapting the FcγR dimers to be included in a multiplex assay, we were capable of analyzing the breadth of FcγR dimer binding to the RV144 Abs produced in response to 32 HIV-1 Ags, including Env Ags that spanned seven different clades, of which several have previously been classified as neutralizing tier 1A, 1B, and tier 2 strains (43). Across the panel of Ags, gp120 proteins were better recognized by vaccinees than gp140 or gp41, a result of the gp120-specific RV144 vaccine regimen and inner domain accessibility. Our results are consistent with those of Bonsignori et al. (42), who tested 21 ADCC mAb isolated from six RV144 vaccine recipients for cross-clade reactivity across subtype A/E, B, and C proteins. Their study recognized strong cross-reactivity with clade B protein Bal and clade A/E protein CM253 but less cross-reactivity for clade C proteins. Our breadth analysis using individual whole anti-HIV Ab repertoires also recognized a strong RV144 cross-clade reactivity to clade B proteins BaLgp120, JRCSFgp120, and 63521gp120 as well as across A/E proteins CM235gp120, and 93TH975gp120, which is expected due to the prime and boost with A/E proteins, but surprisingly we also saw that several vaccinees had strong recognition of several different clade C ENV proteins as well (e.g., C-1086gp120/140).

The cross-clade binding patterns of RV144-generated Abs to FcγRIIIa-V158 compared with FcγRIIa-H131 were broadly similar, but also had some key differences. Interestingly, FcγRIIIa-V158 binding Abs recognize a different breadth pattern of HIV Ags compared with FcγRIIa-H131 binding Abs; this could be attributed to their differing affinities (19), as evident in Supplemental Fig. 2A and 2B, which clearly displays differently clustered Ags for each FcγR. The cross-reactivity for SF162-gp140 trimer is interesting as it further reinforces evidence that gp140-trimer has high antigenicity. Although it has been shown to induce potent neutralizing Ab responses (44, 45), in this study we identify it as a target of FcγR-binding Abs as well.

A unique analysis included in this study was the identification that RV144 vaccinees with higher anti-V1V2 Ab recognition, which was identified as a correlate of protection (4), was also associated with increased breadth of FcγR binding recognition. This suggests anti-V1V2 Ab recognition may potentially be a surrogate marker of potentially protective increased FcγR binding-functional breadth, which was previously suggested by the V1V2 breadth sieve analysis (46). Exploring this in greater detail in future vaccines is warranted. Interestingly, our analyses detected strong responses to C-1086gp120/gp140, which is one of the protein Ags (gp120) included in the recently initiated HVTN702 vaccine trial in South Africa (20). Given the strong cross-reactivity to this Ag in the RV144 trial, it will be interesting to examine the breadth of FcγR-binding Ab responses induced by this new vaccine regimen to obtain a more nuanced picture of vaccine immunogenicity and, potentially, protective capacity (41).

A limitation of this novel FcγR-binding assay is that it remains a proxy for functional information. Although the FcγR dimer–binding assay correlated well with various analyses of the commonly used RFADCC cell-based assay, further correlations with other functional ADCC assays will be useful. Additionally, the FcγR dimer binding is, as expected, significantly more sensitive for FcγRIIIa-V158 and FcγRIIa-H131 variants than the lower affinity FcγRIIIa-F158 variant, which is a common variant (9). We acknowledge that the correlations between the functional RFADDC assays and our Fc cross-linking Ab ELISA assays are modest (r values 0.46–0.72); however, we note that functional ADCC assays can be variable due to the requirement for cultured effector and target cells. Indeed, in the recently published comparison of seven separate functional ADCC and ADCP assays for the VAX004 HIV vaccine trial (22), there were only three significant positive correlations (all between $p = 0.01$–0.05 and r values <0.5) among the 21 unadjusted correlations performed between these functional assays. In previous analyses of the RV144 trial samples, although different markers of Ab-induced NK cell activation correlated well with each other, correlations between NK cell activation, ADCC, and ADCP were modest, with r values of 0.2–0.46 (6). This illustrates the diversity of responses in functional outcomes and difficulties achieving very high correlations with an Fc cross-linking Ab ELISA assay and any given functional assay.

In conclusion, this study identifies the presence of FcγR-binding Abs induced by the RV144 vaccine regimen. In general, the RV144-induced FcγR binding Abs recognized a modest number of HIV-1 Env proteins; however, higher breadth correlated strongly with strong anti-V1V2 Abs. In the future, these novel high-throughput assays could also be adapted to detect FcγR function against other infectious diseases (38) and across various animal models, including the generation of macaque FcγR dimers that could be used to assess preclinical HIV vaccines. Ultimately, it will be important to correlate our Fc cross-linking Ab ELISA assay with the results of human HIV vaccine efficacy trials such as the recently initiated HVTN702 trial. This assay has the potential to focus investigations and reduce the need to run cell-based assays for the early recognition of ADCC and ADCP functional Abs, and so accelerate the identification of immune responses that may contribute to an effective HIV-1 vaccine.

Acknowledgments

We sincerely thank S. Rerks-Ngarm, P. Pitisuttithum, S. Nitayaphan, J. Kaewkungal, J.H. Kim, N.L. Michael, and the entire RV144 team of investigators for generously providing the critical RV144 samples. We also thank all the volunteers who participated in this landmark trial. We acknowledge the generosity of the National Institutes of Health AIDS reagents program, which shared several HIV protein Ags used in these studies.

Disclosures

The authors have no financial conflicts of interest.

References

1. UNAIDS. 2016. Global Aids Update 2016. UNAIDS, Geneva, Switzerland, p. 14.
2. Cox, R. J. 2013. Correlates of protection to influenza virus, where do we go from here? *Hum. Vaccin. Immunother.* 9: 405–408.
3. Rerks-Ngarm, S., P. Pitisuttithum, S. Nitayaphan, J. Kaewkungwal, J. Chiu, R. Paris, N. Premsri, C. Namwat, M. de Souza, E. Adams, et al; MOPH-TAVEG Investigators. 2009. Vaccination with ALVAC and AIDSVAX to prevent HIV-1 infection in Thailand. *N. Engl. J. Med.* 361: 2209–2220.
4. Haynes, B. F., P. B. Gilbert, M. J. McElrath, S. Zolla-Pazner, G. D. Tomaras, S. M. Alam, D. T. Evans, D. C. Montefiori, C. Karnasuta, R. Sutthent, et al. 2012. Immune-correlates analysis of an HIV-1 vaccine efficacy trial. *N. Engl. J. Med.* 366: 1275–1286.
5. Zolla-Pazner, S., A. deCamp, P. B. Gilbert, C. Williams, N. L. Yates, W. T. Williams, R. Howington, Y. Fong, D. E. Morris, K. A. Soderberg, et al. 2014. Vaccine-induced IgG antibodies to V1V2 regions of multiple HIV-1 subtypes correlate with decreased risk of HIV-1 infection. *PLoS One* 9: e87572.
6. Chung, A. W., M. Ghebremichael, H. Robinson, E. Brown, I. Choi, S. Lane, A. S. Dugast, M. K. Schoen, M. Rolland, T. J. Suscovich, et al. 2014. Polyfunctional

Fc-effector profiles mediated by IgG subclass selection distinguish RV144 and VAX003 vaccines. *Sci. Transl. Med.* 6: 228ra38.
7. Yates, N. L., H. X. Liao, Y. Fong, A. deCamp, N. A. Vandergrift, W. T. Williams, S. M. Alam, G. Ferrari, Z. Y. Yang, K. E. Seaton, et al. 2014. Vaccine-induced Env V1-V2 IgG3 correlates with lower HIV-1 infection risk and declines soon after vaccination. *Sci. Transl. Med.* 6: 228ra39.
8. Chung, A. W., M. Navis, G. Isitman, L. Wren, J. Silvers, J. Amin, S. J. Kent, and I. Stratov. 2011. Activation of NK cells by ADCC antibodies and HIV disease progression. *J. Acquir. Immune Defic. Syndr.* 58: 127–131.
9. Forthal, D. N., E. E. Gabriel, A. Wang, G. Landucci, and T. B. Phan. 2012. Association of Fcγ receptor IIIa genotype with the rate of HIV infection after gp120 vaccination. *Blood* 120: 2836–2842.
10. Wren, L. H., A. W. Chung, G. Isitman, A. D. Kelleher, M. S. Parsons, J. Amin, D. A. Cooper, I. Stratov, M. Navis, and S. J. Kent, ADCC study collaboration investigators. 2013. Specific antibody-dependent cellular cytotoxicity responses associated with slow progression of HIV infection. *Immunology* 138: 116–123.
11. Lu, J., J. Chu, Z. Zou, N. B. Hamacher, M. W. Rixon, and P. D. Sun. 2015. Structure of FcγRI in complex with Fc reveals the importance of glycan recognition for high-affinity IgG binding. *Proc. Natl. Acad. Sci. USA* 112: 833–838.
12. Lu, J., J. L. Ellsworth, N. Hamacher, S. W. Oak, and P. D. Sun. 2011. Crystal structure of Fcγ receptor I and its implication in high affinity γ-immunoglobulin binding. *J. Biol. Chem.* 286: 40608–40613.
13. Chung, A. W., E. Rollman, R. J. Center, S. J. Kent, and I. Stratov. 2009. Rapid degranulation of NK cells following activation by HIV-specific antibodies. *J. Immunol.* 182: 1202–1210.
14. Clement, M. V., P. Haddad, A. Soulie, J. Guillet, and M. Sasportes. 1990. Involvement of granzyme B and perforin gene expression in the lytic potential of human natural killer cells. *Nouv. Rev. Fr. Hematol.* 32: 349–352.
15. Nagarajan, S., S. Chesla, L. Cobern, P. Anderson, C. Zhu, and P. Selvaraj. 1995. Ligand binding and phagocytosis by CD16 (Fc gamma receptor III) isoforms. Phagocytic signaling by associated zeta and gamma subunits in Chinese hamster ovary cells. *J. Biol. Chem.* 270: 25762–25770.
16. Takasugi, J., Y. Koide, and M. Takasugi. 1977. Reconstitution of natural cell-mediated cytotoxicity with specific antibodies. *Eur. J. Immunol.* 7: 887–892.
17. Mullazehi, M., L. Mathsson, J. Lampa, and J. Rönnelid. 2006. Surface-bound anti-type II collagen-containing immune complexes induce production of tumor necrosis factor alpha, interleukin-1beta, and interleukin-8 from peripheral blood monocytes via Fc gamma receptor IIA: a potential pathophysiologic mechanism for humoral anti-type II collagen immunity in arthritis. *Arthritis Rheum.* 54: 1759–1771.
18. Barouch, D. H., J. Liu, H. Li, L. F. Maxfield, P. Abbink, D. M. Lynch, M. J. Iampietro, A. SanMiguel, M. S. Seaman, G. Ferrari, et al. 2012. Vaccine protection against acquisition of neutralization-resistant SIV challenges in rhesus monkeys. *Nature* 482: 89–93.
19. Hogarth, P. M., and G. A. Pietersz. 2012. Fc receptor-targeted therapies for the treatment of inflammation, cancer and beyond. *Nat. Rev. Drug Discov.* 11: 311–331.
20. Wang, Z., C. Lorin, M. Koutsoukos, D. Franco, B. Bayat, Y. Zhang, A. Carfi, S. W. Barnett, and F. Porter. 2016. Comprehensive characterization of reference standard lots of HIV-1 subtype C Gp120 proteins for clinical trials in Southern African regions. *Vaccines (Basel)* 4: 1–14.
21. Ackerman, M. E., Y. Huang, G. Alter, G. Ferrari, D. Forthal, J. Kappes, G. Lewis, J. Love, L. Harris, B. Borate, et al. 2013. Comparative evaluation of assays for Fc receptor-mediated antibody effector functions targeting HIV-1. In *AIDS Vaccine*. ePostersOnline, Barcelona. Available at: http://epostersonline.com/aidsvax2013/?q=node/1567.
22. Huang, Y., G. Ferrari, G. Alter, D. N. Forthal, J. C. Kappes, G. K. Lewis, J. C. Love, B. Borate, L. Harris, K. Greene, et al. 2016. Diversity of antiviral IgG effector activities observed in HIV-infected and vaccinated subjects. *J. Immunol.* 197: 4603–4612.
23. Montefiori, D. C. 2014. Neutralizing antibody assays for HIV-1, SIV and SHIV: recent advances in technology. In *HIV sequence database*. Laboratory for AIDS Vaccine Research & Development Duke University Medical Center, Durham, NC.
24. Memarnejadian, A., C. E. Meilleur, D. M. Mazzuca, I. D. Welch, and S. M. Haeryfar. 2016. Quantification of alloantibody-mediated cytotoxicity in vivo. *Transplantation* 100: 1041–1051.
25. Valiathan, R., J. E. Lewis, A. B. Melillo, S. Leonard, K. H. Ali, and D. Asthana. 2012. Evaluation of a flow cytometry-based assay for natural killer cell activity in clinical settings. *Scand. J. Immunol.* 75: 455–462.
26. Zaritskaya, L., M. R. Shurin, T. J. Sayers, and A. M. Malyguine. 2010. New flow cytometric assays for monitoring cell-mediated cytotoxicity. *Expert Rev. Vaccines* 9: 601–616.
27. Gómez-Román, V. R., R. H. Florese, L. J. Patterson, B. Peng, D. Venzon, K. Aldrich, and M. Robert-Guroff. 2006. A simplified method for the rapid fluorometric assessment of antibody-dependent cell-mediated cytotoxicity. *J. Immunol. Methods* 308: 53–67.
28. Forthal, D. N., and G. Landucci. 1998. In vitro reduction of virus infectivity by antibody-dependent cell-mediated immunity. *J. Immunol. Methods* 220: 129–138.
29. Forthal, D. N., G. Landucci, and E. S. Daar. 2001. Antibody from patients with acute human immunodeficiency virus (HIV) infection inhibits primary strains of HIV type 1 in the presence of natural-killer effector cells. *J. Virol.* 75: 6953–6961.
30. Vanderven, H. 2016. What lies beneath: antibody dependent natural killer cell activation by antibodies to internal influenza virus proteins. *EBioMedicine*. 8: 277–290.
31. Pollara, J., L. Hart, F. Brewer, J. Pickeral, B. Z. Packard, J. A. Hoxie, A. Komoriya, C. Ochsenbauer, J. C. Kappes, M. Roederer, et al. 2011. High-throughput quantitative analysis of HIV-1 and SIV-specific ADCC-mediating antibody responses. *Cytometry A* 79: 603–612.
32. Wren, L., M. S. Parsons, G. Isitman, R. J. Center, A. D. Kelleher, I. Stratov, N. F. Bernard, and S. J. Kent. 2012. Influence of cytokines on HIV-specific antibody-dependent cellular cytotoxicity activation profile of natural killer cells. *PLoS One* 7: e38580.
33. Madhavi, V., L. H. Wren, R. J. Center, C. Gonelli, W. R. Winnall, M. S. Parsons, M. Kramski, S. J. Kent, and I. Stratov. 2014. Breadth of HIV-1 Env-specific antibody-dependent cellular cytotoxicity: relevance to global HIV vaccine design. *AIDS* 28: 1859–1870.
34. Miller, A. S., M. L. Tejada, and H. Gazzano-Santoro. 2012. Development of an ELISA based bridging assay as a surrogate measure of ADCC. *J. Immunol. Methods* 385: 45–50.
35. Ackerman, M. E., M. Crispin, X. Yu, K. Baruah, A. W. Boesch, D. J. Harvey, A. S. Dugast, E. L. Heizen, A. Ercan, I. Choi, et al. 2013. Natural variation in Fc glycosylation of HIV-specific antibodies impacts antiviral activity. *J. Clin. Invest.* 123: 2183–2192.
36. Brown, E. P., K. G. Dowell, A. W. Boesch, E. Normandin, A. E. Mahan, T. Chu, D. H. Barouch, C. Bailey-Kellogg, G. Alter, and M. E. Ackerman. 2017. Multiplexed Fc array for evaluation of antigen-specific antibody effector profiles. *J. Immunol. Methods* 443: 33–44.
37. Wines, B. D., H. A. Vanderven, S. E. Esparon, A. B. Kristensen, S. J. Kent, and P. M. Hogarth. 2016. Dimeric FcγR ectodomains as probes of the Fc receptor function of anti-influenza virus IgG. *J. Immunol.* 197: 1507–1516.
38. Kristensen, A. B., W. N. Lay, F. Ana-Sosa-Batiz, H. A. Vanderven, V. Madhavi, K. L. Laurie, L. Carolan, B. D. Wines, M. Hogarth, A. K. Wheatley, et al. 2016. Antibody responses with Fc-mediated functions after vaccination of HIV-infected subjects with trivalent influenza vaccine. *J. Virol.* 90: 5724–5734.
39. Kramski, M., A. Schorcht, A. P. Johnston, G. F. Lichtfuss, S. Jegaskanda, R. De Rose, I. Stratov, A. D. Kelleher, M. A. French, R. J. Center, et al. 2012. Role of monocytes in mediating HIV-specific antibody-dependent cellular cytotoxicity. *J. Immunol. Methods* 384: 51–61.
40. Brown, E. P., A. F. Licht, A. S. Dugast, I. Choi, C. Bailey-Kellogg, G. Alter, and M. E. Ackerman. 2012. High-throughput, multiplexed IgG subclassing of antigen-specific antibodies from clinical samples. *J. Immunol. Methods* 386: 117–123.
41. Montefiori, D. C., C. Karnasuta, Y. Huang, H. Ahmed, P. Gilbert, M. S. de Souza, R. McLinden, S. Tovanabutra, A. Laurence-Chenine, E. Sanders-Buell, et al. 2012. Magnitude and breadth of the neutralizing antibody response in the RV144 and Vax003 HIV-1 vaccine efficacy trials. *J. Infect. Dis.* 206: 431–441.
42. Bonsignori, M., J. Pollara, M. A. Moody, M. D. Alpert, X. Chen, K.-K. Hwang, P. B. Gilbert, Y. Huang, T. C. Gurley, D. M. Kozink, et al. 2012. Antibody-dependent cellular cytotoxicity-mediating antibodies from an HIV-1 vaccine efficacy trial target multiple epitopes and preferentially use the VH1 gene family. *J. Virol.* 86: 11521–11532.
43. Seaman, M. S., H. Janes, N. Hawkins, L. E. Grandpre, C. Devoy, A. Giri, R. T. Coffey, L. Harris, B. Wood, M. G. Daniels, et al. 2010. Tiered categorization of a diverse panel of HIV-1 Env pseudoviruses for assessment of neutralizing antibodies. *J. Virol.* 84: 1439–1452.
44. Kovacs, J. M., J. P. Nkolola, H. Peng, A. Cheung, J. Perry, C. A. Miller, M. S. Seaman, D. H. Barouch, and B. Chen. 2012. HIV-1 envelope trimer elicits more potent neutralizing antibody responses than monomeric gp120. *Proc. Natl. Acad. Sci. USA* 109: 12111–12116.
45. Yasmeen, A., R. Ringe, R. Derking, A. Cupo, J. P. Julien, D. R. Burton, A. B. Ward, I. A. Wilson, R. W. Sanders, J. P. Moore, and P. J. Klasse. 2014. Differential binding of neutralizing and non-neutralizing antibodies to native-like soluble HIV-1 Env trimers, uncleaved Env proteins, and monomeric subunits. *Retrovirology* 11: 41.
46. Rolland, M., P. T. Edlefsen, B. B. Larsen, S. Tovanabutra, E. Sanders-Buell, T. Hertz, A. C. deCamp, C. Carrico, S. Menis, C. A. Magaret, et al. 2012. Increased HIV-1 vaccine efficacy against viruses with genetic signatures in Env V2. *Nature* 490: 417–420.

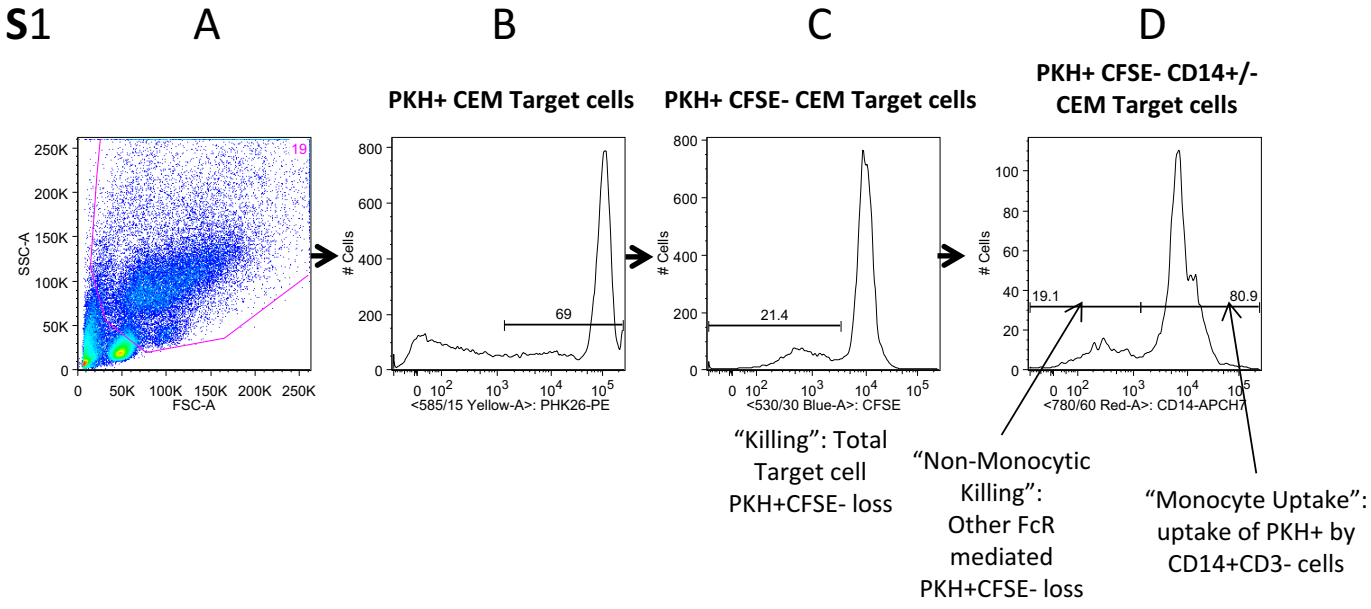

Figure.S1 Gating strategy use to identify ADCC activity as measured by modified Rapid Fluorometric ADCC (RFADCC) Assay. CEM-NKR-CCR5 target cells were identified by FSC vs SSC. CEM Target cells were than selected by gating upon PKH26+ cells. From these PKH26+ CEM cells RFADCC activity was determined as measured by gating upon CFSE- cells. Total RFADCC activity was further delineated as monocyte (CD14+) associated PKH+CFSE- uptake of target cells (38) or CD14- negative "non-monocytic killing" (eg NK cells) FcR mediated PKH+CFSE- loss of target cells.

S2

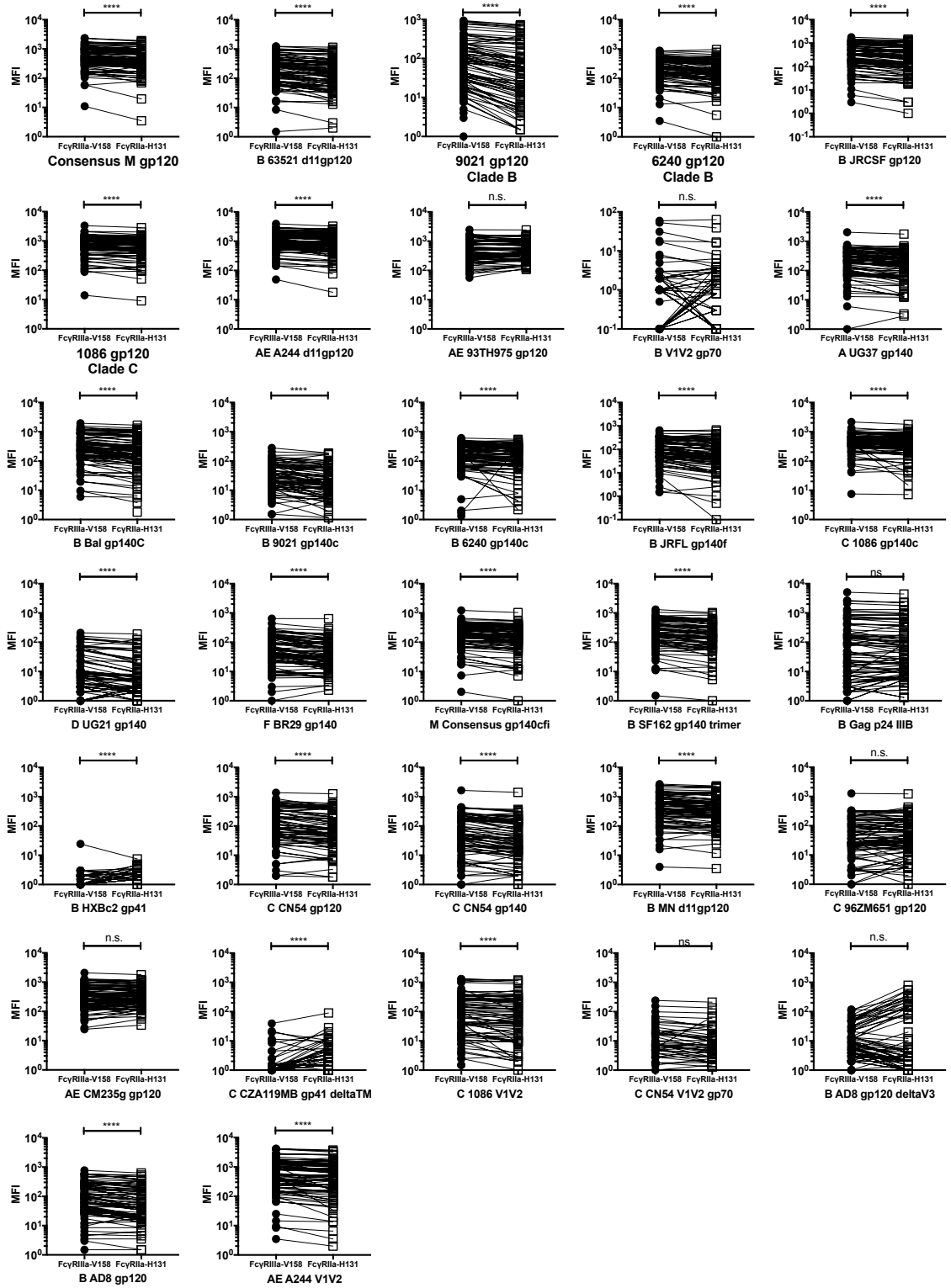

Figure S2. 31 HIV-1 Env antigens paired analyses between FcγRIIIa-V158 and FcγRIIa-H131 binding week 26 vaccinees (n=80). Paired Wilcoxon test used to compare FcγR binding and p-value significance was adjusted with Brodmann's multiple comparisons correction.

S3A

FcγRIIIa-V158

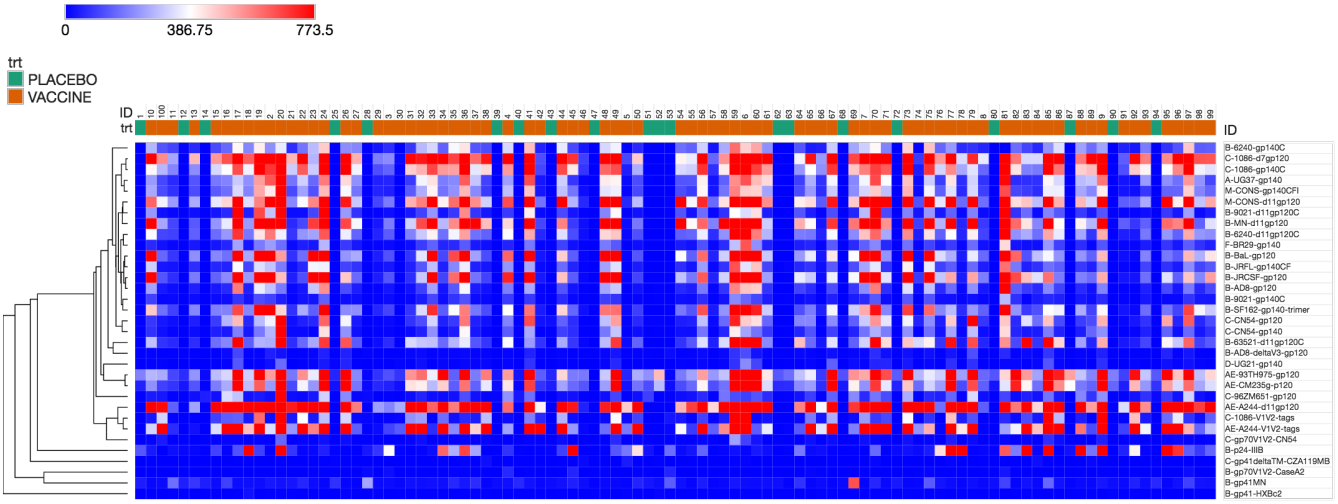

S3B

FcγRIIa-H131

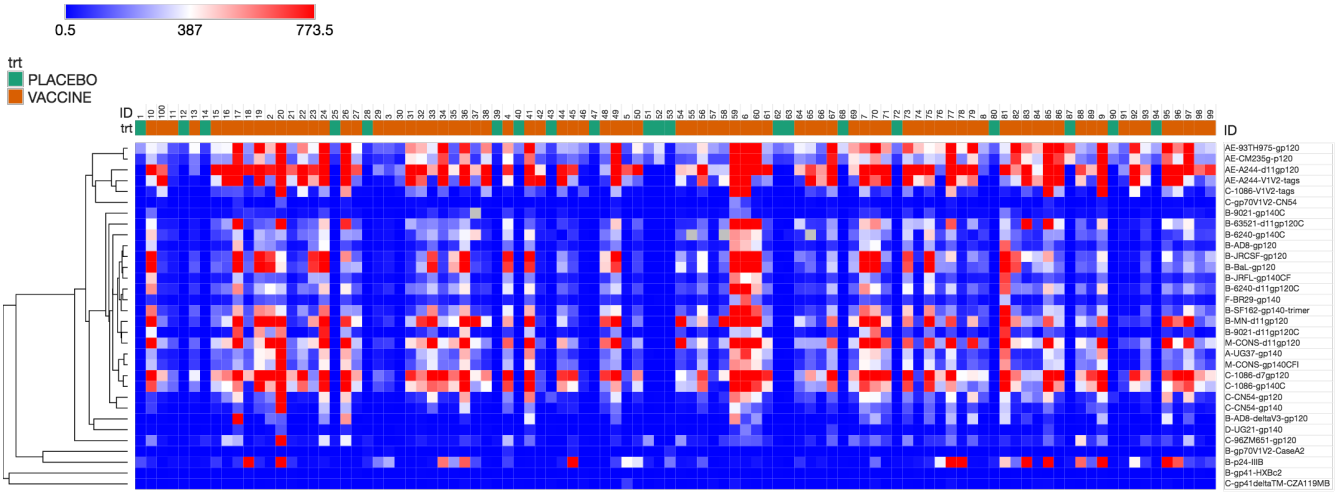

Figure S3. RV144 FcγRIIIa-V158 (A) and FcγRIIa-H131 (B) Ab binding protein breadth analyses. Multiplex assay testing validation RV144 cohort plasma binding FcγRIIIa-V158 specific for different proteins from clades A, B, C, A/E, M and F. Proteins antigens are listed on the right y-axis with hierarchical clustering displayed on the left y-axis.

S4

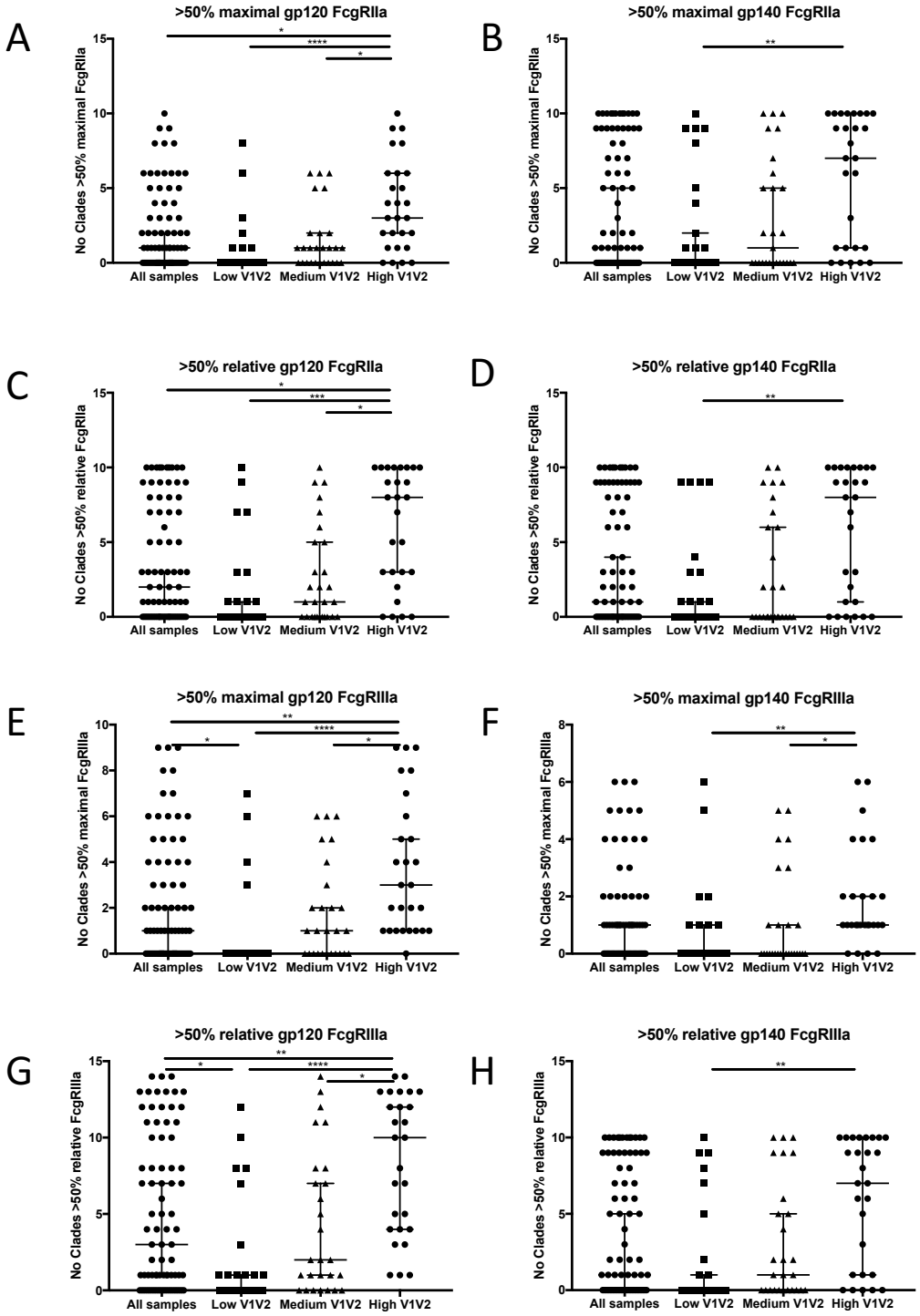

Figure S4. Stronger V1V2 specific antibody FcγR binding association with enhanced breadth
RV144 FcγRIIa-H131 (A-D) and FcγRIIIa-V158 (E-H) antibody binding responses were standardised by z-score and were separated into those that had low, medium and high V1V2 responses (V1V2-responses separated into tertiles). Maximal FcγRIIa (A) and FcγRIIIa (E) binding of different gp120 proteins was determined by comparing all FcγR responses to all gp120 proteins and identifying the strongest antigen (A244 gp120 for both FcγRs). Thus >50% maximal was determined by identifying which subjects had FcgR above 50% of the identified maximal response for each antigen. The same analysis was repeated examining only gp140 proteins for FcγRIIa (B) and FcγRIIIa (F). Relative FcγRIIa (C,D) and FcγRIIIa (G,H) binding was determined by identifying individually for each HIV antigen which subjects had FcγR >50% of the relative maximum binding response for each antigen, with analysis separated into examining exclusively gp120 antigens (C,G) and gp140 antigens (D,H).